 doi:10.20944/preprints202205.0305.v1

Article

Occurrence of Lymphangiogenesis in Peripheral Nerve Autografts Contrasts Schwann Cell-induced Apoptosis of Lymphatic Endothelial Cells *in vitro*

Carina Hromada[1,2], Jaana Hartmann[2,3], Johannes Oesterreicher[2,3], Anton Stoiber[2,3], Anna Daerr[1,2], Barbara Schädl[2,3], Eleni Priglinger[2,3], Andreas H. Teuschl-Woller[1,2], Wolfgang Holnthoner[2,3], Johannes Heinzel[3,4] and David Hercher[1,2,3*]

[1] Department Life Science Engineering, University of Applied Sciences Technikum Wien, Vienna, Austria
[2] Austrian Cluster for Tissue Regeneration
[3] Ludwig Boltzmann Institute for Traumatology, The Research Centre in Cooperation with AUVA, Vienna, Austria
[4] Department of Hand-, Plastic, Reconstructive and Burn Surgery, BG Unfallklinik Tuebingen, University of Tuebingen, Germany
* Correspondence: David.Hercher@trauma.lbg.ac.at

Abstract:

Peripheral nerve injuries pose a major clinical concern world-wide, and functional recovery after segmental peripheral nerve injury is often unsatisfactory, even in case of autografting. Although it is well established that angiogenesis plays a pivotal role during nerve regeneration, the influence of lymphangiogenesis is strongly underinvestigated. In this study, we analyzed the presence of lymphatic vasculature in healthy and regenerated murine peripheral nerves, revealing that nerve autografts contained increased numbers of lymphatic vessels after segmental damage. This led us to elucidate the interaction between lymphatic endothelial cells (LECs) and Schwann cells (SCs) *in vitro*. We show that SC and LEC secretomes do not influence the respective other cell types' migration and proliferation in 2D scratch assay experiments. Furthermore, we successfully created lymphatic microvascular structures in SC-embedded 3D fibrin hydrogels in the presence of supporting cells, whereas SCs seemed to exert anti-lymphangiogenic effects when cultured with LECs alone. Here, we describe for the first time increased lymphangiogenesis after peripheral nerve injury and repair. Furthermore, our findings indicate a potential lymph-repellent property of SCs, thereby providing a possible explanation for the lack of lymphatic vessels in the healthy endoneurium. Our results highlight the importance to elucidate the molecular mechanisms of SC-LEC interaction.

Keywords: peripheral nerve regeneration, lymphangiogenesis, Schwann cells, lymphatic endothelial cells

1. Introduction

Peripheral nerve injuries pose a major clinical concern world-wide, affecting up to 60,000 in 1,000,000 individuals every year [1], [2]. Moreover, 20 million people are estimated to be suffering from some form of neuropathy in the US alone, resulting in approximately $150 billion of annual health care costs for the treatment, care and rehabilitation of patients, mainly caused by the low success rate of both, spontaneous and surgical peripheral nerve repair [1]–[4]. The consequences pose a major socioeconomic burden due to significant deterioration or even persisting disability of patients associated with loss of sensory and/or motor function and unemployability, thereby strongly devastating the patients' quality of life [3], [5], [6]. Moreover, peripheral nerve damage often leads to

 doi:10.20944/preprints202205.0305.v1

neuropathic pain, a serious condition affecting 6-8% of the population and accounting for 20-25% of all chronic pain disorders [7]–[9].

The peripheral nervous system has a remarkable regenerative capacity, which can be mainly attributed to the Schwann cells' remarkable plasticity, allowing them to adopt a regeneration-promoting repair phenotype. These Schwann cells (SCs) participate in the degradation of myelin by autophagy, attract macrophages, activate neurotrophic factor expression and migrate to form a cellular bridge, called bands of Büngner, to guide regenerating axons [10], [11]. However, if peripheral nerve damage is too severe, the intrinsic regenerative capacity is not sufficient to functionally recover the damaged nerve and surgical interventions become necessary. The current gold standard of surgical treatment options for segmental tissue loss after nerve injury are nerve autografts, but their use has certain limitations: firstly, the limited availability of suitable autologous nerves, and secondly, the occurrence of sensory and/or motor functional deficits at the donor site [11]–[13]. The alternative of decellularized allografts are on the other hand associated with poorer clinical outcomes [13]–[15]. This highlights the clinical relevance of peripheral nerve injuries and the urgent need for improved repair methods.

The success rate of novel therapeutic approaches to treat peripheral nerve defects might be greatly enhanced by advancing our still rather rudimental understanding of the structure and function of the peripheral nerve itself. The anatomy of a nerve is often pictured as a cable-like structure: it consists of myelinated nerve fibers – *i.e.* axons surrounded by SCs – that are enclosed by the endoneurium and bundled into nerve fascicles by the perineurium. The outermost layer of connective tissue called epineurium in turn bundles several fascicles into the entire nerve. It can be further subdivided into the epifascicular epineurium which surrounds the whole nerve trunk and the interfascicular epineurium which spans the space between the individual fascicles [16]. Described first by german anatomist Johannes Lang, but still a matter of scientific debate, is the paraneurium, a layer of loose connective tissue enabling gliding of the nerve trunk [17], [18]. Furthermore, peripheral nerves have a longitudinal extrinsic vascular system surrounding the nerve, which consists of larger vessels to provide blood supply for the epi- and perineurial space, and a longitudinal intrinsic microvascular system for the endoneurial space [19]. While the organization of the blood vasculature of peripheral nerves as well as its importance during peripheral nerve regeneration is well described [20]–[22], studies investigating the anatomy and physiology of the neural lymphatic system are scarce [23]. Prospero Homeobox 1 (Prox-1) has been identified as key molecule for lymphangiogenesis and nerve regeneration following crush injury of the murine sciatic nerve [24]. It has also been shown that the formation of new blood vessels after nerve transection guides migrating Schwann cells to bridge the defect, which in turn guides regenerating axons [21], whereas the role of the lymphatic system in neuropathies has remained widely unexplored to date.

Sir Sidney Sunderland was the first to describe the existence of two distinct lymphatic capillary networks inside peripheral nerves – one in the epineurium and one in the endoneurial compartment, which are separated from each other by the perineurium [25]. However, until the early 2000s, the observation of lymphatic vasculature mainly relied on ultrastructural examinations due to the lack of marker molecules specific for lymphatic vessels. In 2006, Volpi *et al* firstly reported the immunohistochemical identification of lymphatics in the epineurium, but not in the endoneurium, of human sural nerves [26]. Given that peripheral nerve repair is frequently accompanied by endoneurial fibrosis, swelling and local inflammation – all of which represents characteristics of a dysfunctional lymphatic system –, Frueh *et al* recently hypothesized that the lymphatic system plays an essential role during peripheral nerve injury and repair [27]. Frueh *et al* explicitly highlight the immense gap of knowledge regarding the neural lymphatic system and suggest thorough histological investigations peripheral nerve specimens, *in vivo* analysis of lymphangiogenesis of physiological and pathological peripheral nerves, as well as *in vitro* studies to elucidate the interplay between lymphatic endothelial cells and SCs or neuronal cells

 doi:10.20944/preprints202205.0305.v1

[27]. Recently, the same group investigated failed human sensory nerve allografts associated with lack of reinnervation and neuropathic pain, and showed that allograft failure was characterized by increased intraneural fibrosis, abnormal neurofilament organization, increased and randomly distributed blood microvasculature and, most interestingly, scarce lymphatic vasculature compared to healthy nerves [28].

With this study, we aim to provide fundamental insights regarding the role of the lymphatic system after peripheral nerve injury *in vivo* and to elucidate the interplay of lymphatic endothelial cells (LECs) and SCs *in vitro*. After an *in vivo* study of segmental nerve damage with autologous nerve grafting in a rat model, we observed an increase in lymphatic vessels in the nerve graft. This sparked our interest and led us to investigate the interaction between primary SCs and primary LECs in 2D and 3D *in vitro* experiments. Specifically, we investigated the influence of pro-regenerative SCs as well as their secretome on lymphatic vessel formation in 3D fibrin hydrogels and the migration of LECs in a 2D scratch assay, respectively. Taken together, our findings will not only shed light onto the involvement of lymphatic system in injured peripheral nerves, but also pave the way to the establishment of novel therapeutic approaches for improved nerve regeneration.

2. Materials and Methods

2.1 Ethical Approval

The experimental protocol was approved beforehand on July 23rd, 2019, by the Animal Protocol Review Board of the City Government of Vienna (Magistrate's office number 58, Project identification code: MA58-421715-2019-16.) All procedures were carried out in full accord with the Helsinki Declaration on Animal Rights and the Guide for the Care and Use of Laboratory Animals of the National Institutes of Health.

2.2 Animals

Nine male Lewis rats (Janvier Labs, Le Genest-Saint-Isle, France), weighing 280–360 g, underwent bilateral surgical transection of the median nerve with unilateral repair using autologous nerve graft (ANT, n=9). The animals were kept in groups of two or three in appropriate cages with ad libitum access to food and water. Following their arrival at the animal facility, rats were allowed a 7-day acclimatization period before any experimental handling.

2.3 Experimental Surgery

Following acclimatization, rats underwent bilateral median nerve resection as described previously [29]. All surgeries were performed under aseptic conditions using an operation microscope (Leica M651, Leica Microsystems, Vienna, Austria). Anesthesia was maintained by an oxygen-anesthetics mixture (95-98.5% oxygen, 1.5-5% sevoflurane) through inhalation via a nose cone. For sufficient peri- and postoperative anesthesia, buprenorphine (0.05 mg/kg) was injected subcutaneously preoperatively and every 8 hours postoperatively for at least 24 hours. Additionally, Meloxicam (0.75 mg/kg) was applied orally for at least 4 days following surgery. After careful dissection of the surrounding tissue, 7 mm of the left and right median nerve were removed after performing a microsurgical transection about 1.5 mm proximal to the crossing point of the median nerve and brachial artery and vein. Two minutes prior to transection, two drops of 2% lidocaine were applied on the nerve. The second transection was performed 7 mm proximal to the first one. In the right forelimb, the nerve gap was bridged with the original nerve segment in reverse fashion serving as a homotopic nerve autograft, which was coaptated to the nerve stumps with two interrupted sutures per coaptation site (Ethilon R 10-0, Ethicon-Johnson & Johnson, Brussels, Belgium). In the left forelimb, the nerve defect remained unreconstructed and the distal nerve stump was sutured into the short head of the biceps muscle to prevent reinnervation. The subcutaneous tissue and skin were closed with interrupted absorbable sutures (Vicryl 5-0, Johnson & Johnson, Vienna, Austria).

2.4 Tissue preparation for histological analysis

 doi:10.20944/preprints202205.0305.v1

At the end of the 12-week postoperative observational period, animals were sacrificed in deep anesthesia as described before by means of an intracardially applied overdose of sodium thiopental. Immediately following sacrification, a segment of the right median nerve was harvested containing the reconstructed nerve segment as well as 5 mm of the original nerve proximal and distal to it.

To obtain the correct position as well as distal and proximal orientation of the nerves, they were pinned with minutien needles on small Styrofoam stubs. For histochemical and immunohistochemical stainings, the nerves were fixed in 4% buffered formalin for 24 hours at room temperature and afterwards rinsed in tap water for 1 hour. Dehydration with an uprising ethanol series was performed, beginning with 50% EtOH for 1 hour, followed by 70% EtOH. Then, the samples were transferred to a vacuum infiltration processor (Sakura, TissueTek ® VIP) and after further dehydration of the samples, infiltrated with paraffin via the intermedium of xylene. Cutting the nerve samples in 4 µm thin cross-sections was performed with an Microm HM355S (ThermoScientific). After drying the sections overnight in a 37°C oven, the slides were deparaffinized and rehydrated for staining with different methods. Nuclei are stained in grey using Weigert's Iron Heamatoxylin. After staining, the sections are dehydrated and permanently embedded with Shandon Consul-Mount (Thermo Scientific). Starting immunohistochemical stainings, the sections were first pre-treated with different antigen retrieval protocols. For S100 (Agilent, Z0311) the sections were incubated with Pepsin (Sigma) for 10min at 37°C in a humidified chamber. The sections for podoplanin (ReliaTech, 104-M40) staining were steamed in a pH 6 sodium citrate buffer (0.1 M) for 20min, for CD31 (Thermo, PA5-16301) with EDTA buffer (0.1 M) at pH 9. After the antigen retrieval, the sections were blocked using Bloxall® (VectorLabs) for 10 min. Then, the primary antibodies were applied for 1 hour at room temperature (S100 1:1600, podoplanin 1:2000, CD31 1:50) followed by incubation of secondary antibodies for 30 min at room temperature using an HRP conjugated anti-mouse system (ImmunoLogic, VWRKDPVM110HRP) for S100 and podoplanin. For CD31 an anti-rabbit HRP conjugated antibody was used (ImmunoLogic, VWRKDPVR110HRP). The detection of the staining was performed with ImmPACTTM NovaREDTM (VectorLabs). Then the sections were counterstained with Haematoxylin and after dehydration permanently embedded with Shandon Consul-Mount (Thermo Scientific).

2.5 Automated quantification of lymphatic vessels

Automated, deep learning-based image analysis was used to evaluate lymphatic vessels in whole-slide scans of histological cross sections. We adopted the IKOSA platform (KML Vision) to train a state-of-the-art deep convolutional neural network (CNN) model to segment and measure podoplanin-stained vessels in the scans. The trained application provides a set of morphometric parameters that are calculated automatically for each detected object. To improve the quality of data annotations for supervised learning, we used regions of interest (ROI) to restrict the image content and marked the vessels with the annotation tools provided by IKOSA. Similarly, we used ROI to define areas without lymphatic vessels to aid the model distinguishing between foreground and background. A set of 13 scans was randomly split into training (10 images, 233 ROI) and validation (3 images, 42 ROI). Training was performed on GPU-accelerated cloud infrastructure, the semantic segmentation performance was evaluated on the validation set using Dice coefficient, precision and recall metrics, see **supplementary document 1** for more details.

2.6 Cell Culture

SCs were dissected from collected sciatic nerves from adult female and male Lewis rats, according to a protocol modified from Kaekhaw et al [30] and Weiss et al [31]. Briefly, the epineurium was removed from sciatic nerves and nerve fascicles were digested in Dulbecco's Modified Eagle's Medium High Glucose (DMEM HG, Lonza) containing 0.1% Collagenase Type I ((w/v), Sigma Aldrich), 1.25% Dispase I ((w/v), Sigma Aldrich), 3 mM $CaCl_2$, 1% Penicillin/Streptomycin (P/S, Lonza) and 1% Amphotericin at 37°C and 5% CO_2 overnight. The next day, digested fascicles were triturated, the suspension filtered

 doi:10.20944/preprints202205.0305.v1

through a 70 µm nylon cell strainer and DMEM HG (Lonza) supplemented with 10% fetal calf serum (FCS, GE Healthcare) was added. After centrifugation at 300*g* for 5 min, the cell pellet was resuspended in Schwann cell medium consisting of DMEM HG D-Valine (Himedia) supplemented with 10% FCS, 1% P/S, 1% L-Glutamine, 10 ng/ml heregulinβ-1 (PeproTech, #100-03) and 2 µM forskolin (Sigma Aldrich), and seeded onto poly-l-lysine and laminin-coated plates.

LECs were isolated from the dermal microvascular endothelial cell population of human juvenile foreskin, which was obtained with informed consent and ethical approval (Ethic Committee Charité University Medicine, Berlin, Germany) after routine circumcisions, [32]. As previously described [33], LEC were isolated by immunomagnetic cell sorting using anti-podoplanin antibody and magnetic beads (Dynabeads, M280 goat anti-rabbit, Thermo Fisher) according to manufacturer's instructions. The podoplanin-positive LEC were maintained in Endothelial Cell Growth Medium-2 (EGM-2) consisting of Endothelial Cell Basal Medium-2 containing 5% FCS and endothelial growth supplements (EGM-2 Bulletkit, Lonza) as well as 25 ng/ml VEGF-C (ReliaTech). LEC were retrovirally infected with enhanced yellow fluorescent protein (eYFP) to visualize vascular network formation in 3D fibrin hydrogels as described previously [33].

Human adipose-derived stem/stromal cells (ASCs) were isolated from liposuction material as described previously [34] after prior approval by the ethics committee of Upper Austria (ethics vote #200) and maintained in EGM-2.

2.7 2D scratch assay

Schwann cells or LEC were seeded onto 6-wells and grown until confluency in Schwann cell medium or EGM-2, respectively. 24 hours before the experiment, media was exchanged for a 1:1 mixture of Schwann cell medium and EGM-2. The supernatant was then collected and centrifuged at 300*g* for 5 min. In the meantime, the monolayers were scratched with a 1000 µl pipet tip along a ruler to create a gap. After a washing step with 1x Dulbecco's Phosphate Buffered Saline (DPBS, Lonza) to remove floating cells from scratching, SCs and LECs were cultivated in SC-conditioned medium, LEC-conditioned medium, or unconditioned medium for 72 hours. Images were taken at 0, 6, 20, 24, 48, and 72 hours, and closure of the cell-free area was quantified with the "Wound Healing Size Tool" plugin for ImageJ/Fiji® [35]. Three scratch assay experiments with different biological donors were performed with a total of 15 technical replicates for the SC and LEC secretome groups; two scratch assay experiments with different biological donors with a total of 12 technical replicates were performed for the unconditioned media group.

2.8 2D co-cultures

Two-dimensional co-cultures were prepared in 24-well plates with 20,000 cells per cell type in duplicates of the following groups: (i) YFP-LEC + ASC + SC, (ii) YFP-LEC + SC, and (iii) YFP-LEC + ASC. Cultures were maintained in a 1:1 mixture of Schwann cell medium and EGM-2 supplemented with 25 ng/ml VEGF-C for 7 days, and media was exchanged every 2-3 days. Images were acquired with a Leica DMI6000B epifluorescence microscope.

2.9 Cultivation of cells in 3D fibrin hydrogels

Fibrin hydrogels containing different compositions of SCs, YFP-LECs and ASCs were prepared as previously described [33]. Briefly, 100,000 YFP-LECs were embedded either (i) alone, together (ii) with 100,000 SCs and 100,000 ASCs (LEC + ASC + SC), (iii) with 100,000 SCs only (LEC + SC), or (iv) with 100,000 ASCs only (LEC + ASC) in 200 µl fibrin hydrogels on 15-mm round glass coverslips with a final concentration of 2.5 mg/ml fibrin and 0.2 U/ml thrombin (Tissucol Duo, Baxter). After polymerization at 37°C and 5% CO_2 for 15 minutes, a 1:1 mixture of Schwann cell medium and EGM-2, supplemented with 25 ng/ml VEGF-C and 100 U/ml aprotinin was added to fibrin hydrogels. Each hydrogel-cell composition was prepared in quadruplicate, of which 2 hydrogels each were stimulated with 10 ng/ml TNF-α for the first 48 hours. Media exchanges were performed every 2-3

 doi:10.20944/preprints202205.0305.v1

days. Four independent experiments were performed with three different biological donors for SCs, and two different biological donors for both, YFP-LECs and ASCs. SCs were used between passage 4 and 7, whereas YFP-LECs and ASCs were used between passages 6 and 9.

2.10 Immunostaining of 3D fibrin hydrogels

3D fibrin hydrogels were fixed on day 7 in 4% formaldehyde (ROTI Histofix, Carl Roth) for 20 min at room temperature. After three washing steps in DPBS, hydrogels were blocked and permeabilized in DPBS containing 1% bovine serum albumin (BSA, Sigma Aldrich), 3% goat serum and 0.1% Triton X-100 (Sigma Aldrich) for 30 min at room temperature. To stain Schwann cells, hydrogels were incubated in rabbit polyclonal anti-S100 antibody (1:400, DAKO Agilent, Z0311) in DPBS with 1% BSA, 3% goat serum and 0.1% Triton X-100 at 4°C overnight. After three washing steps in DPBS, hydrogels were incubated in goat anti-rabbit AlexaFluor 594 secondary antibody (1:400, ThermoFisher Scientific) in DPBS with 1% BSA, 3% goat serum and 0.1% Triton X-100 at 37°C for 1 hour. After another three washes in DPBS, nuclei were counterstained with DAPI (1:1000), hydrogels again washed three times in DPBS and mounted with Fluoroshield (Sigma Aldrich) on glass slides. Images were taken at three representative areas of each fibrin hydrogel using a Leica THUNDER Imager Live Cell & 3D Assay microscope. Selected samples were scanned with a TissueFAXS tissue cytometer (TissueFAXS version 7.1.6245.112, TissueGnostics GmbH, Vienna, Austria).

2.11 Vascular network quantification

Lymphatic vascular networks were quantified using the open source tool Angiotool [36]. Main readout parameters were percentage of network vs total area, total tubule length and number of junctions.

2.12 Timelapse imaging of 2D co-cultures

2.12.1 Nanolive imaging

SCs were first stained with Vybrant DiD Cell-Labeling Solution (Thermo Fisher Scientific). Following incubation of 20 minutes at 37°C and 5% CO_2, the labeling solution was removed from the cells through centrifugation at 300*g* for5 min and subsequently washed once with PBS. YFP-LECs and the DiD labeled SCs were seeded 100,000 cells per cell type to one μ-Dish 35 mm, low (ibidi Gmbh, Gräfeling, Germany) in a total volume of 1 mL. The cells were maintained in a 1:1 mixture of Schwann cell medium and EGM-2, supplemented with 25 ng/mL VEGF-C. Before imaging could commence, the cells were incubated for 1.5 hours at 37 °C and 5 % CO_2 in order to be allowed to settle and adhere. After incubation, imaging of the sample with the 3D Cell Explorer (Nanolive SA, Tolochenaz, Switzerland) began. The sample was observed for a duration of 48 hours. A brightfield image was acquired every 6 frames, while a fluorescence image was collected every 7 frames. YFP-LECs and SCs were used at passage 6 and 8, respectively.

2.12.2 JuLI imaging

SCs and YFP-LECs were seeded 10,000 cells per cell type to one well of a 48-well plate (Thermo Fischer Scientific) in a total volume of 500 μL. The cells were maintained in a 1:1 mixture of Schwann cell medium and EGM-2, supplemented with 25 ng/mL VEGF-C. After seeding, the co-culture sample was incubated at 37 °C and 5 % CO_2 for 2 hours in order to be allowed to settle and adhere. Over the span of 48 hours, images were collected every 30 minutes in brightfield, fluorescence, and merged versions with a JuLI Smart fluorescent cell analyzer (NanoEnTek Inc, Seol, Korea). YFP-LECs and SCs were used between passage 6 and 9.

2.12 Statistical Analysis

Statistical analyses were performed with GraphPad Prism 9 and data are presented as mean ± standard deviation. Unless indicated differently, all data were evaluated using One-Way ANOVA with Tukey post tests to perform multiple comparisons.

 doi:10.20944/preprints202205.0305.v1

3. Results

3.1 Autologous Nerve Grafts Show Increased Numbers Of Lymphatic Vessels

In order to investigate the role of the lymphatic system in pathophysiological settings after segmental nerve damage, we screened for the presence of lymphatic vessels in healthy and injured median nerves. Immunohistochemical analysis revealed a significantly increased number and total area of podoplanin-positive vessels in the mid-graft section of the autologous nerve transplant when compared to the proximal section (**Figure 1**). Training the CNN model took about 12 minutes, resulting in an overall dice score of 0.86, precision of 91.54%, and recall of 80.74% on the validation dataset. The model is robust and does not confuse blood vessels with lymphatic vessels. For a detailed performance report of the automated evaluation for each individual ROI please refer to **supplementary document 1**. In contrast, in healthy median nerves no lymphatic vessels were found (data not shown), indicating a potential role of lymphatics in peripheral nerve regeneration but not homeostasis.

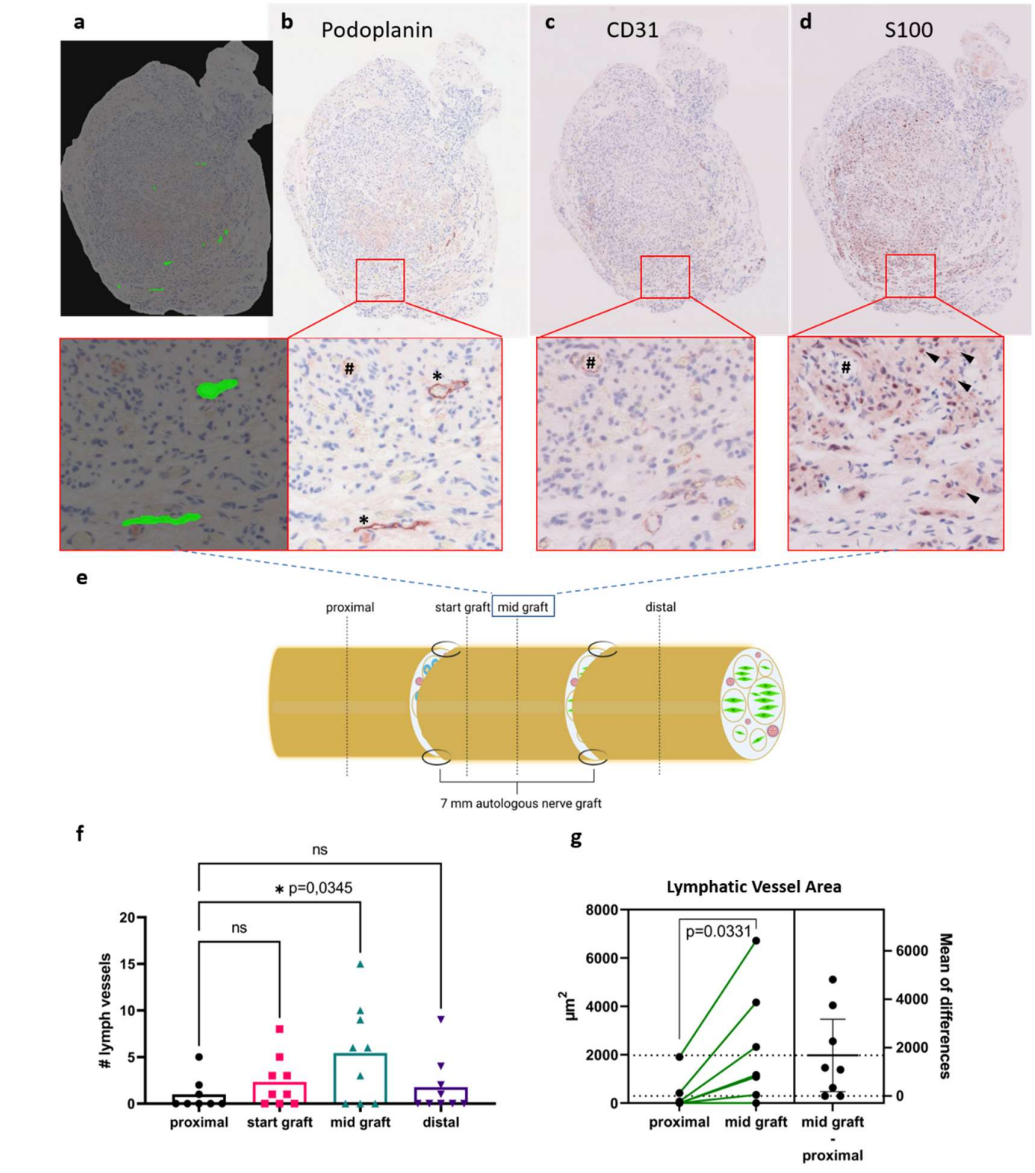

Figure 1. Autologous nerve grafting results in increased intraneural lymphangiogenesis. a-d) Histological cross sections at mid-graft level in a rat median defect model 3 months after autologous nerve grafting. a) Readout of the automated identification using KML Vision IKOSA deep learning

 doi:10.20944/preprints202205.0305.v1

algorithm, lymphatic vessels are highlighted in green, b) staining for podoplanin reveals lymphatic vessels in the regenerate (indicated with asterisks (*) in the magnified picture), c) staining for the endothelial marker CD31 identified blood vessels (corresponding vessel is indicated in b-c with "#") and staining for S100 the distribution of Schwann cells (selected myelinating and non-myelinating Schwann cells are indicated with arrowheads). e) schematic of the repaired median nerve with histological sections and their respective localization indicated as proximal, start graft, mid graft and distal. f) quantification of podoplanin+ lymphatic vessels in the histological sections show a significantly higher number of lymphatic vessels at mid graft level, when compared to the proximal nerve section. g) determination of lymphatic vessel area of individual nerves shows a significant increase from proximal to mid graft with a mean difference of observed area of approx. 1800 μm^2 (ns - not significant, $p<0.05$ was considered significant)

3.2 Secretomes of Schwann cells and lymphatic endothelial cells do not influence each others capacity to close cell monolayer gaps

Since we observed an increased number of lymphatic vessels in autologous nerve grafts after segmental nerve damage, we aimed to investigate the interaction between primary SCs and LECs in *in vitro* settings. In a first step, we performed *in vitro* scratch assay experiments to analyze the effect of SC and LEC secretomes on cell migration and proliferation. Therefore, confluent LEC and SC monolayers were scratched with a 1000 µl pipet tip to create a cell-free area and scratched cell monolayers were either incubated with conditioned media derived from LECs or SCs, or with unconditioned medium to serve as a control. Although SC migration was slightly slower with SC secretome compared to unconditioned medium or LEC secretome, this effect was not statistically significant (**Figure 2**A, C). Similarly, there was a trend towards slower cell migration and/or proliferation of LECs when cultivated in LEC secretome compared to SC secretome or unconditioned medium, which was statistically non-significant (**Figure 2**B, D).

Overall, gap closure was achieved by both cell types with no significant difference in cell migration and proliferation between conditioned media of either LEC or SC and unconditioned media for both cell types.

Preprints (www.preprints.org) | NOT PEER-REVIEWED | Posted: 23 May 2022 doi:10.20944/preprints202205.0305.v1

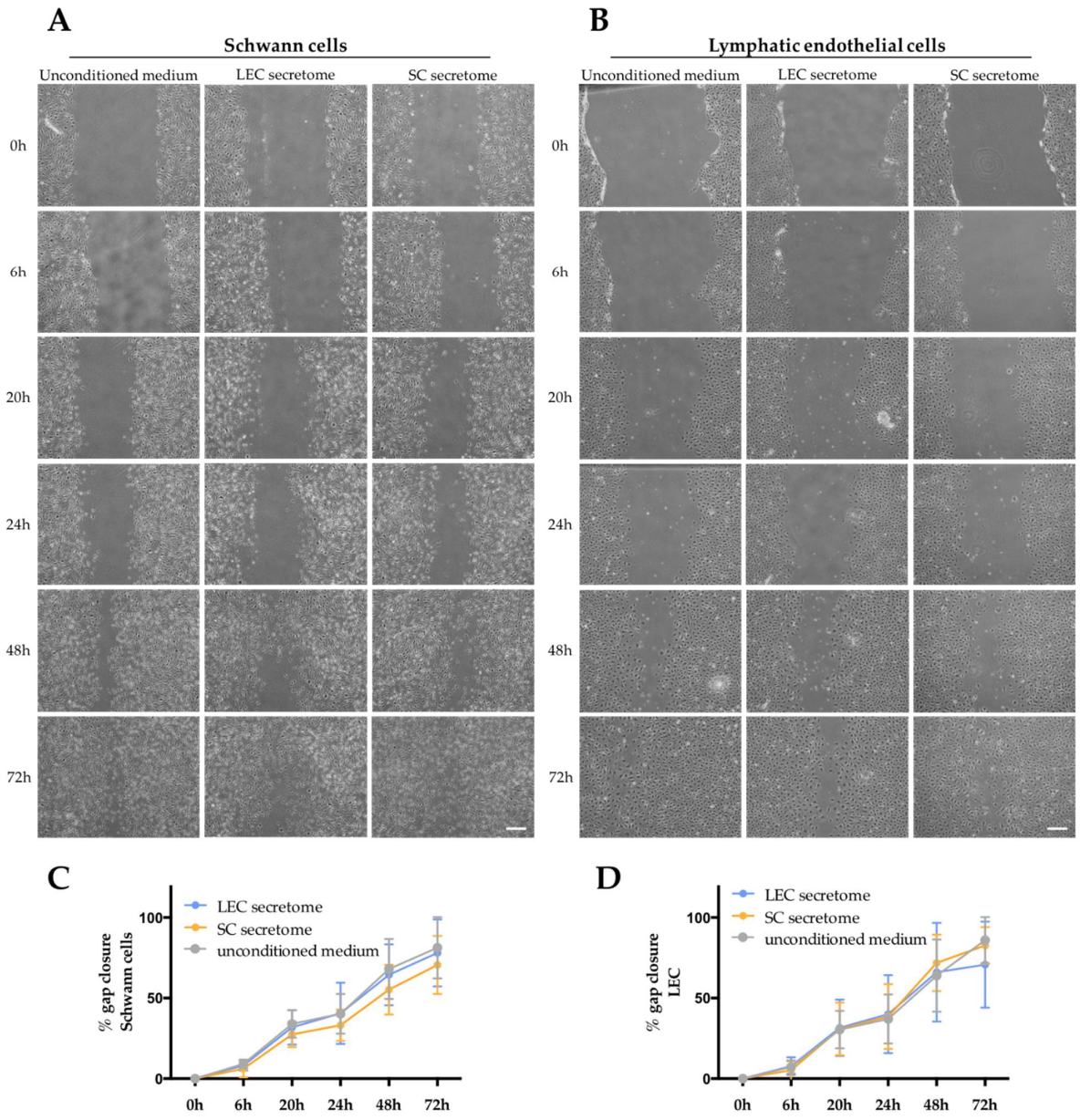

Figure 2. Schwann cell migration was not altered by lymphatic endothelial cell secretome in 2D scratch assay experiments. A, B) SCs and LECs were grown until confluency and their conditioned media was collected 24 hours before the experiment. Scratches were created on cell monolayers and cell migration in either unconditioned medium or conditioned medium from LEC or SC was monitored over a total of 72 hours. Scale bars = 300 µm. C, D) Quantification of gap closure shows that the secretome of LECs and SCs does not affect migration of either SCs or LECs. Data are presented as mean ± sd. LEC secretome and SC secretome: n=15 of 3 independent experiments; unconditioned medium: n=12 of 2 independent experiments.

3.3 2D Cultures of LEC, SC and ASC induce the formation of lymphatic vascular structures

We next aimed to examine the influence of SCs on lymphatic tube morphogenesis in 2D cultures. Previous observations showed that LEC are able to form a vascular network when co-cultured with ASCs as a supporting cell type in 2D as well as 3D cultures [33]. Here, we aimed to determine whether LECs can also form networks when co-cultured either with SCs only or with both, ASCs and SCs in 2D within seven days. Both the co-

 doi:10.20944/preprints202205.0305.v1

culture with ASCs and the tri-culture with ASCs and SCs resulted in the formation of elongated and interconnected vascular-like networks (**Figure 3**). However, LEC were not able to form tube-like structures and moreover appeared to decrease in number when cultured together with SC only.

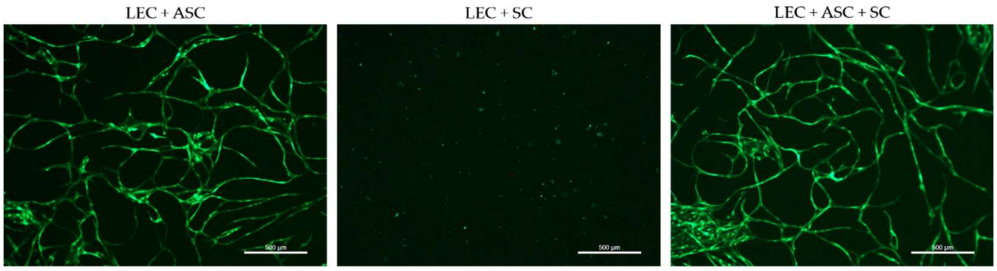

Figure 3. 2D culture of YFP-LECs with either ASCs or SCs alone, or with both ASCs and SCs. Cells were seeded in equal densities. Elongated lymphatic network-like structures formed when LECs were co-cultured with ASCs as well as with both, ASCs and SCs. In contrast, LECs remained as single cells but also seemed to decrease in number when cultured with SCs alone. Scale bars = 500 µm.

3.4 3D Cultivation of LEC and SC in presence of ASC induces the formation of lymphatic vessel-like structures in fibrin hydrogels

In order to investigate the influence of SCs on lymphatic vessel formation in a more physiologically relevant setting, LECs were integrated into 3D fibrin hydrogels either as monocultures, as co-cultures with either ASCs or SCs alone, or as tricultures with both, ASCs and SCs (**Figure 4**). LECs formed highly dense and interconnected lymphatic networks in the presence of ASCs, which serve as a supporting cell type for vessel formation. Even though a lymphatic network also formed in tri-cultures with both, ASCs and SCs, this network was less dense and interconnected as compared to the co-culture with ASCs only. In accordance with the observations from the 2D experiments, LECs failed to develop vascular structures when embedded into fibrin matrices with SCs only and remained as single cells, indicating that SCs do not serve as a supporting cell type that enables tube-like formation of LECs. However, when LECs were cultivated alone, primitive elongated tube-like structures could form, whereas LECs appeared mostly round when co-cultured with SCs only, indicating that SCs might induce apoptosis on LECs.

Preprints (www.preprints.org) | NOT PEER-REVIEWED | Posted: 23 May 2022 doi:10.20944/preprints202205.0305.v1

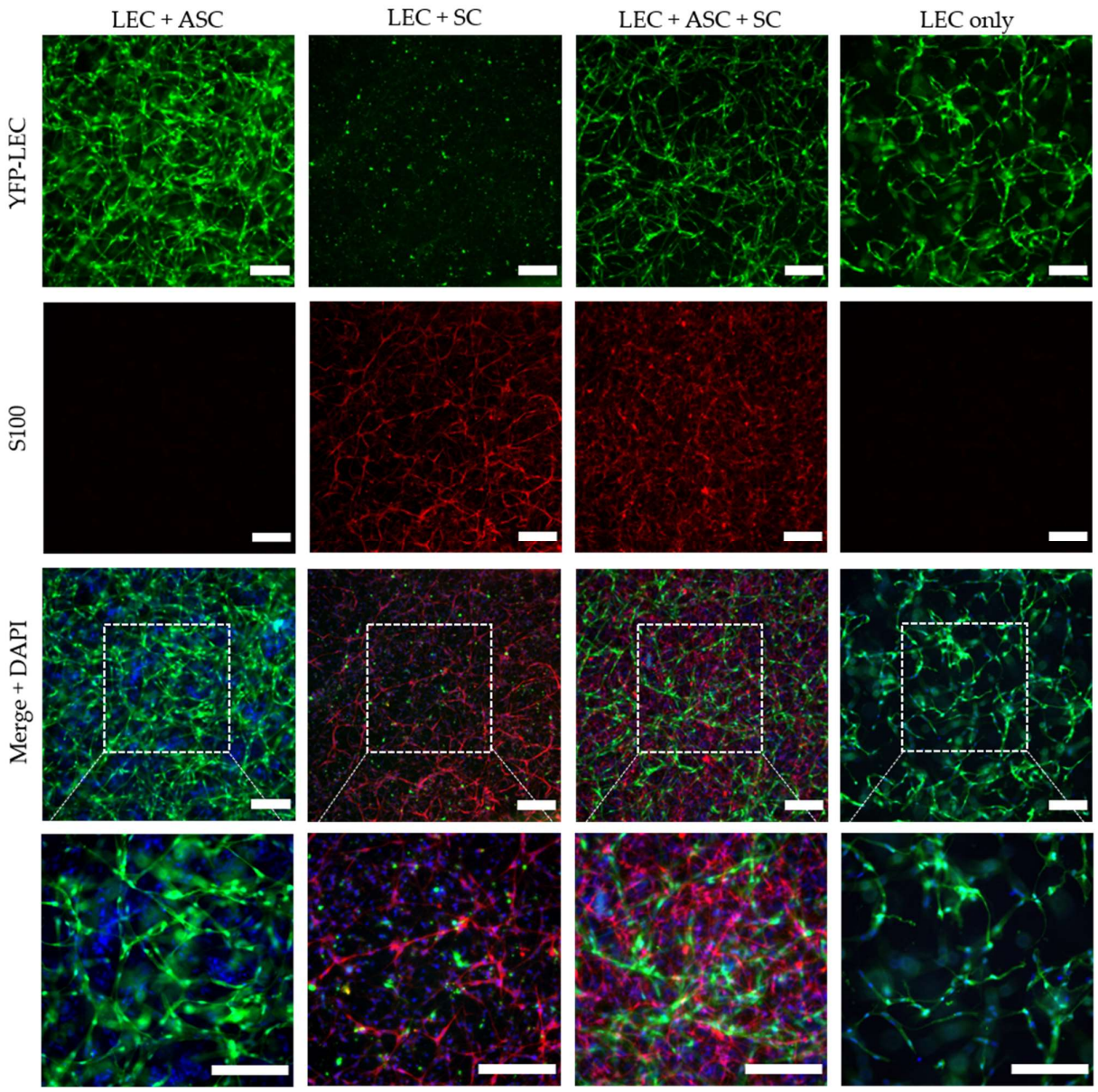

Figure 4. Lymphatic network formation is decreased in presence of Schwann cells in 3D fibrin hydrogels. LEC formed elongated and interconnected networks when cultivated with ASC as a supporting cell type (LEC+ASC). In a tri-culture of LECs, ASCs and SCs, lymphatic vessel formation was less dense and interconnected (LEC+ASC+SC), whereas in the monoculture of LECs, only primitive tube-like structures were formed. In contrast, co-culture of only LECs and SCs inhibited the formation of lymphatic tubes. Green – LECS, red – SCs stained against S100, blue – cell nuclei. Scale bars = 200 μm.

The quantification of network parameters showed a significantly larger area covered with lymphatic networks, higher numbers of junctions as well as longer tubule length in the co-culture of LECs with ASCs compared to the tri-culture of LECs with ASCs and SCs (**Figure 5**). However, the higher network density in LEC and ASC co-cultures might also be attributed to the fact that a lower total cell number was embedded into fibrin hydrogels compared to tri-culture hydrogels, thereby giving the vessel-like structures more space to spread and occupy.

 doi:10.20944/preprints202205.0305.v1

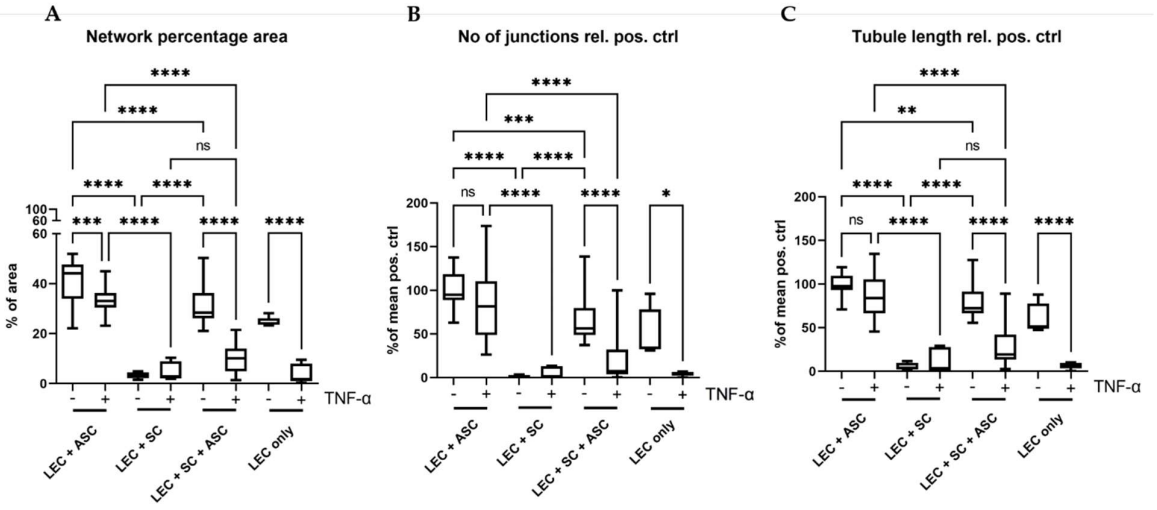

Figure 5. Quantification of the formed lymphatic networks in 3D fibrin clots. In all parameters, the triple culture of LECs, SCs and ASCs showed significantly lower levels than the positive control (LEC+ASC). Co-culture of LECs with SCs inhibited network formation, whereas addition of ASCs reversed this effect. Furthermore, also the effect of pro-inflammatory TNF-α on the formation of lymphatic networks was evaluated. Here, we observed a larger negative effect of TNF-α on the triple-culture when compared to the positive control in all parameters. LEC+ASC, LEC+SC and LEC+ASC+SC: n=8 each of 4 independent experiments, LEC only: n=4 of 2 independent experiments. *p<0.05, **p<0.01, ***p<0.001, ****p<0.0001, ns not significant.

To evaluate whether SCs induce apoptosis in a paracrine manner, we cultivated fibrin hydrogels containing either LECs only or a co-culture of LECs and ASCs in SC-conditioned medium (unconditioned medium served as a control). When cultivated in SC-conditioned medium, LECs did not form elongated tube-like structures and grew in distinct clusters, thereby indicating a paracrine effect of SCs on LECs. This effect was less pronounced when LECs were cultivated with ASCs, suggesting that ASCs are able to ameliorate this SC-induced effect (Supplementary Figure 1).

In order to more closely elucidate how LECs are dying in co-culture with SCs, we performed 2D co-cultures, which were then used for timelapse imaging using two different systems, the JuLI (Supplementary Figure 2) as well as the Nanolive system. We observed induction of apoptotic cell death of LECs over a time period of several hours, resulting in almost complete clearance of LECs in the co-culture within 48h. The high resolution Nanolive imaging indicates a cell-cell contact induced apoptosis within 5h of co-culture (**Figure 6**). In particular, SCs extended filopodia-like protrusions towards LECs, eventually resulting in apoptosis of LECs as indicated by the formation of LEC-derived apoptotic bodies (**Figure 6**f). Upon LEC death, SCs again retract their filopodia-like protrusions. Timelapse videos are provided in Supplementary Videos 1-3.

 doi:10.20944/preprints202205.0305.v1

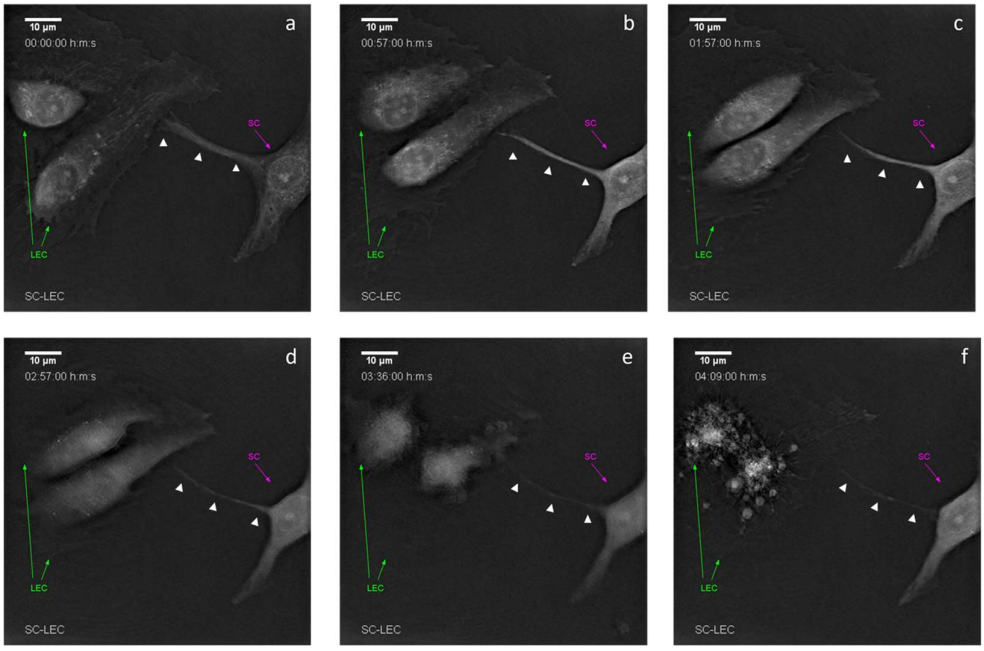

Figure 6: Live cell imaging demonstrates cell-cell contact induced lymphatic endothelial cell death by Schwann cells. a) Initial cell-cell contact between lymphatic endothelial cells (LEC, green arrow) and Schwann cells (SC, magenta arrow) via filopodia-like protrusions (white arrow heads). b) After initial contact, morphological changes in both LEC and the SC-filopodia-like protrusions become visible. c, d) Retraction of both the filopodia-like protrusion and LEC endoplasm. e) Stark retraction and compartmentalization of LEC. f) Formation of LEC-derived apoptotic bodies. Time-lapse shown in each image is the observation time starting 2h post-seeding.

Interestingly, when SCs were cultivated with LECs and ASCs, SCs sometimes assembled into several islands, which were surrounded by lymphatic vascular structures (**Figure 7**).

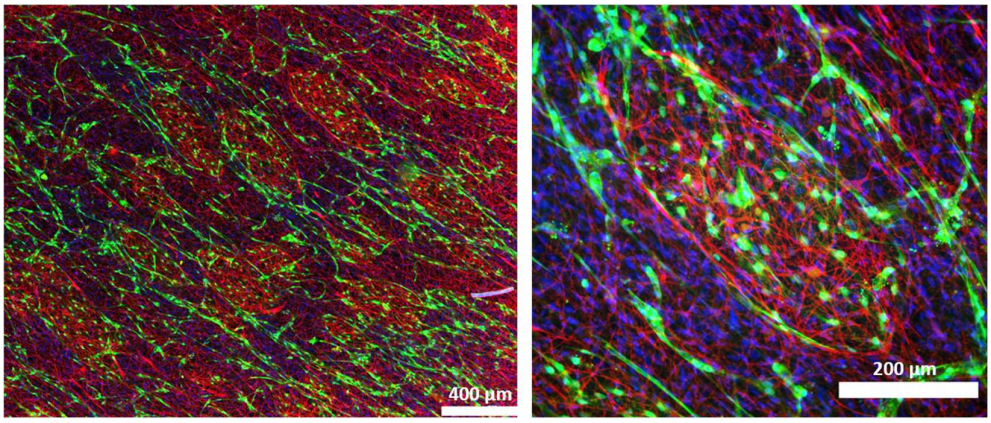

Figure 7. Schwann cells (red) assemble into islands, which are surrounded by lymphatic vessels (green) in co-cultures of LECs, ASCs and SCs. Green – LECS, red – SCs stained against S100, blue – cell nuclei. Scale bar = 200 µm.

3.5 Stimulation of 3D fibrin hydrogel cultures with TNF α impairs lymphatic network formation

Considering that peripheral nerve regeneration and neuropathies in general are associated with an inflammatory environment, we next aimed to evaluate the influence of the pro-inflammatory cytokine TNF-α on Schwann cell behavior as well as lymphatic network development. LEC were embedded into 3D fibrin hydrogels either as monocultures,

 doi:10.20944/preprints202205.0305.v1

or together with ASC, with SC, or with ASC and SC, and stimulated with 10 ng/ml TNF-α for 48 hours. Regarding lymphatic network formation, LEC formed more interconnected and dense networks when cultivated with ASC alone compared to the triculture with both ASC and SC, whereas in co-culture with SC and in LEC monocultures, lymphatic vessel development was again completely inhibited (**Figure 8**). However, compared to 3D cultures that have not been stimulated with TNF-α (**Figure 4**), lymphatic network formation was generally less pronounced under inflammatory conditions. This might indicate the importance of a compromised lymphatic system during chronic inflammatory neuropathies. The quantification of network parameters showed a significantly smaller area covered with lymphatic networks when LECs were cultivated alone, together with ASCs, or together with ASCs and SCs when stimulated with TNF-α (**Figure 5**A). Furthermore, stimulation with TNF-α also resulted in fewer junctions as well as shorter tubule length in LEC single cultures and co-cultures of LECs, ASCs, and SCs (**Figure 5**B, C). Comparison of all TNF-α cultures revealed a significantly larger area covered with lymphatic networks, higher numbers of junctions as well as longer tubule length in the co-culture of LECs with ASCs compared to the tri-culture of LECs with ASCs and SCs, or the co-culture with SCs (**Figure 5**).

 doi:10.20944/preprints202205.0305.v1

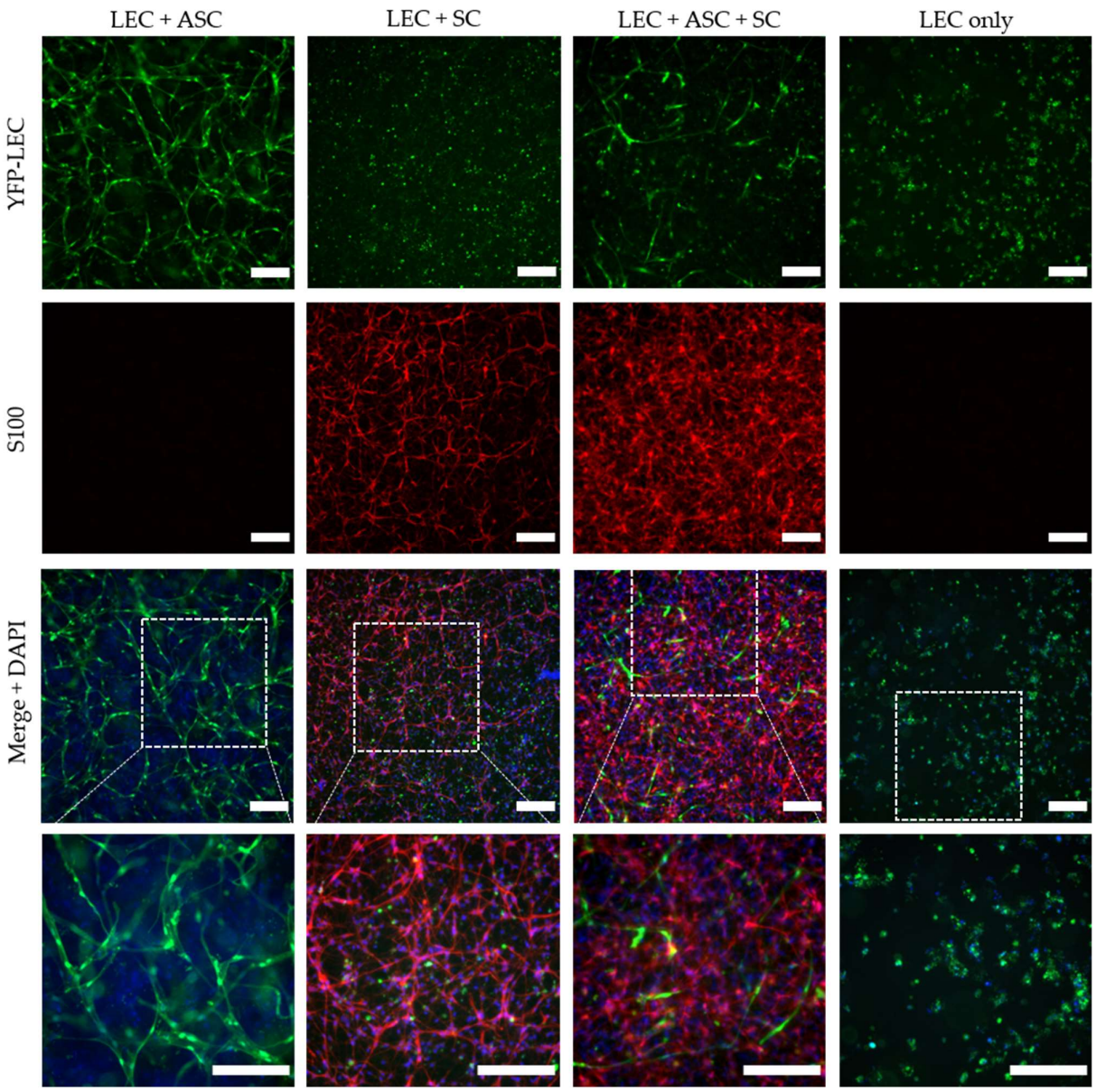

Figure 8. Schwann cells hinder lymphatic vascular network formation in the presence of the pro-inflammatory cytokine TNF-α. LEC + ASC formed elongated and interconnected networks even when stimulated with TNF-α, whereas the formation of lymphatic vessel-like structures in the LEC + ASC + SC cultures in the presence of TNF-α was hampered. The co-culture of only LECs and SCs did not show the formation of lymphatic tubes. Green – LECS, red – SCs stained against S100, blue – cell nuclei. Scale bars = 200 μm.

Interestingly, stimulation with TNF-α also induced changes in SC morphology, especially when cultured together with LEC and ASC. In the presence of TNF-α, SCs manifest a multipolar morphology with highly branched protrusions (**Figure 9**). This phenotype was not observed in unstimulated cultures.

 doi:10.20944/preprints202205.0305.v1

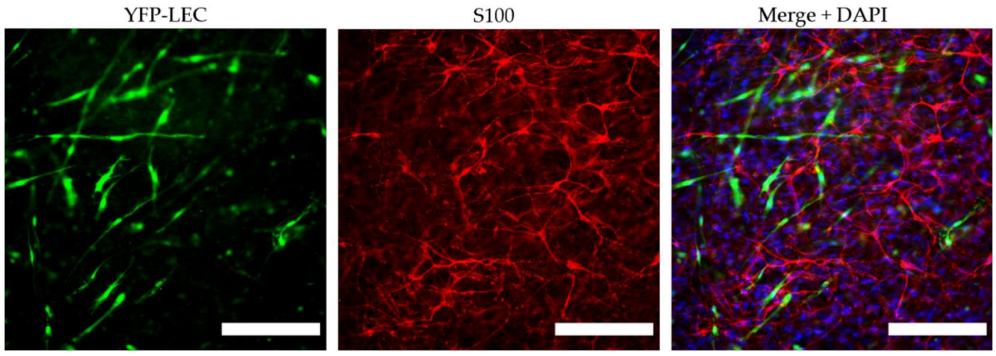

Figure 9. TNF-α induces phenotypical changes in Schwann cells. Stimulation with TNF-α resulted in a morphological change of SC from a bipolar to a multipolar phenotype with highly branched protrusions. Green – LECS, red – SCs stained against S100, blue – cell nuclei. Scale bars = 200 µm.

4. Discussion

Although a functional lymphatic system for peripheral nerve regeneration is likely important for peripheral nerve repair, the influence of lymphangiogenesis during nerve regeneration has largely uninvestigated. In this study, we identified the presence of lymphatic vessels in autologous nerve transplants after segmental median nerve damage, whereas healthy median nerves were void of lymphatic vasculature. Aiming to more closely analyze the interaction between SCs and LECs *in vitro*, we furthermore found that LEC and SC secretomes did not influence cell migration and proliferation. Moreover, lymphatic microvascular structures were successfully created in SC-embedded 3D fibrin hydrogels in the presence of ASCs as a supporting cell type, whereas SCs inhibited lymphangiogenesis when cultured with LECs only.

Peripheral nerve injuries pose a major clinical concern world-wide, and functional recovery after peripheral nerve injury using nerve grafts is still far from satisfactory. Although it is well established that angiogenesis plays a pivotal role during nerve regeneration [21], the importance of the lymphatic system during peripheral nerve injury and repair has only been hypothesized. The fact that a damaged lymphatic system results in persistent swelling and inflammation due to compromised tissue drainage, both of which is frequently observed after the use of nerve grafts, highlights the urgent need of a more thorough investigation of the lymphatic system in peripheral nerves in both, physiological and pathophysiological settings. Moreover, it has been shown that during embryogenesis, the blood and lymphatic vascular and peripheral nervous system share molecular cues that guide both, axonal growth cones as well as vascular tip cells during vessel formation, especially class 3 semaphorins [37], [38]. Here, we observed lymphatic vessels in autologous nerve grafts after segmental damage of the median nerves, while lymphatic vascular structures were absent in healthy median nerves. This might indicate that a functional lymphatic system is required for peripheral nerve repair, but not for the homeostasis of the peripheral nervous system. Observations supporting this theory were published by Meng et al. in 2020 who identified Prox-1 as a key protein not only in regard to the formation of new lymphatic vessels but also nerve regeneration following sciatic crush injury in a rat model. The authors emphasized the importance of this newly formed lymphatic vasculature for the reduction of tissue edema necessary to restore the nerve's functionality [24]. Based on these observations *in vivo*, we aimed to elucidate the interaction between SCs and LECs *in vitro.* First, we performed 2D scratch assay experiments to assess whether the cells' secretome affects migration of LECs and SCs after creating a cell-free area by scratching confluent LEC and SC monolayers; however, there only seemed to be a slight trend that cell migration was slower when cultivated in its respective conditioned medium compared to unconditioned medium as well as the other cells' secretome. Since SC-conditioned medium did not impact LEC migration, we continued to analyze the effect of

 doi:10.20944/preprints202205.0305.v1

SCs on lymphatic vessel formation through direct contact, first in 2D experiments and subsequently in 3D fibrin cultures. ASCs were used as a supporting cell type for lymphatic vessel formation, since we have previously shown that ASCs promote lymphatic tube formation in 2D as well as 3D cultures [33] and it has also been reported that lymphangiogenesis is supported by secretion of factors such as angiopoietin-1, VEGF-A and -D, fibroblast growth factor 2 and hepatocyte growth factor [39]. Within a period of only 7 days, LECs co-cultured with ASCs and SCs formed elongated and interconnected networks that were, however, less dense than those of the positive control (LEC + ASC). To further investigate the reduced lymphatic network density in tri-cultures of LECs, ASCs and SCs, the addition of another cell type into the positive control hydrogels (LEC + ASC) would be important to determine whether this effect is related to an increased cell density within the hydrogel. Additionally, Landau *et al* recently reported that cultivation of LECs with fibroblasts failed to induce lymphatic vessel formation and hypothesized that the inhibition of vessel formation was due to the production of dense collagen layers and excessive tension present in these cultures [40]. Consequently, to screen for the presence of different extracellular matrix (ECM) proteins and the potential differences thereof between the different cultures would allow to identify a potential correlation between ECM secretion and lymphangiogenesis.

Interestingly, when LECs were cultivated with SCs only not even primitive tube-like structures could be formed in 3D fibrin hydrogels. Furthermore, we observed an altered LEC morphology when cultivated in SC-conditioned medium, resulting in a less elongated morphology, cell clustering and the absence of even primitive elongated tube-like structures, indicating at least partly a paracrine effect of SCs on LECs. The fact that this effect was nevertheless not as prominent as in a direct co-culture of LECs with SCs, on the one hand indicates that it is rather a combined paracrine and juxtacrine effect of SCs on LECs, and on the other hand that ASCs as a supporting cell type are able to ameliorate this effect. Consequently, to identify the molecular mechanisms involved in this process, the analysis of differential expression of pro- *versus* anti-lymphangiogenic genes and proteins in triple-cultures of LECs, ASCs and SCs compared to co-cultures of LECs and ASCs would be of high relevance. For example, Huang *et al* showed that SCs produce anti-angiogenic molecules and identified high levels of tissue inhibitor of metalloproteinase-2 (TIMP-2) as well as low levels of pigment epithelium-derived factor (PEDF) – both known inhibitors of angiogenesis – in SC supernatants [41], [42]. However, in contrast to our observations, they also observed an inhibitory effect of SC-conditioned medium specifically on blood endothelial cell proliferation and migration [41], [42]. In another study, the same group identified secreted protein acidic and rich in cysteine (SPARC) as another essential anti-angiogenic molecule expressed and secreted by SCs, which not only inhibited blood endothelial cell migration but also induced apoptosis *in vitro*, and furthermore suppressed angiogenesis *in vivo*, the effects of which could be fully reversed by the addition of neutralizing anti-SPARC antibody [43]. Moreover, SPARC seemed to inhibit lymphangiogenesis in ovarian cancer through reduced VEGF-C and -D expression [44]. These findings suggest that several factors expressed by SCs act synergistically to inhibit the formation of vasculature. Indeed, we also observed an increased amount of SPARC present in the supernatant of LEC + SC fibrin hydrogels on day 7 compared to the other hydrogel groups (data not shown), indicating that the anti-lymphangiogenic effect might be at least in part caused by the secretion of SPARC.

Another interesting observation was the assembly of SCs into distinct islands, which were enclosed by lymphatic vessels. Hence, to analyze cell-cell interactions between SCs and LECs might provide important insights into the role of lymphatic vessels for SC guidance as well as the influence of SC organization on lymphatic vessel assembly.

Since peripheral nerve injuries and neuropathies are accompanied by inflammation, we aimed to assess the influence of the pro-inflammatory cytokine TNF-α on lymphatic network formation as well as on SC behavior. Stimulation with TNF-α not only resulted in reduced lymphatic vessels present in all cultures, but also induced an altered SC

morphology with multiple highly branched and very long protrusions, especially when cultured with ASCs and LECs.

Although we here firstly describe the interaction between SCs and lymphatics *in vitro*, our study has two main limitations. Firstly, we used a physiologically non-representative combination of cells in our *in vitro* experiments, *i.e.* the use of LECs and ASCs derived from human material together with SCs isolated from rat nerves due to the limited availability of human nerve tissue. Hence, it would be an interesting option to perform the experiments presented in our study with SCs derived from human induced pluripotent stem cells to confirm that the results are reproducible in a fully human system. Secondly, this is a primarily descriptive study lacking further analyses to elucidate underlying mechanisms. Apart from the analysis of pro- and anti-lymphangiogenic genes already mentioned above, especially the gene expression profiles of cells in the different fibrin hydrogel cultures to assess (i) the influence of LECs on SC phenotype, and (ii) the influence of stimulation with TNF-α on SC phenotype remain to be elucidated.

Overall, our study highlights the feasibility to engineer lymphatic vessels in the presence of SCs, which paves the way for the generation of more complex tissue engineered constructs, comprising Schwann cells, neuronal cells as well as blood and lymphatic endothelial cells. Such peripheral nerve-like tissue with separate blood and lymphatic vascular networks are desperately needed as biomimetic *in vitro* models to adequately study neuropathies, neurotoxic effects of drugs, as well as peripheral nerve regeneration.

Supplementary Materials: The following supporting information can be downloaded at: www.mdpi.com/xxx/s1, Figure S1: title; Table S1: title; Video S1: title.

Author Contributions: Conceptualization, D.H., J.H. and W.H.; methodology, C.H., B.S., A.S., A.D. and J.O.; writing—original draft preparation, C.H.; writing—review and editing, C.H., E.P., J.H., J.O., D.H. and A.T.; visualization, C.H. and J.O.; supervision, D.H., A.T. and W.H.; project administration, D.H.; funding acquisition, D.H., A.T., W.H. and J.H. All authors have read and agreed to the published version of the manuscript.

Funding: This research was funded by the City of Vienna, grant number MA23 #30-10 and MA23 #30-11 and the Lorenz Böhler Fonds 6_20.

Institutional Review Board Statement: The animal study protocol was approved by the Ethics Committee of the Ludwig Boltzmann Institute for Traumatology. The experimental protocol was approved beforehand by the Animal Protocol Review Board of the City Government of Vienna. All procedures were carried out in full accordance with the Helsinki Declaration on Animal Rights.

Data Availability Statement: All data underlying this study included in the manuscript and the supplementary material. Original data will be provided upon request

Acknowledgments: We would like to thank Katharina Schimek (Technische Universität Berlin) for the human dermal microvascular endothelial cells, as well as the experimental surgery team of the LBI for Traumatology for their support in conducting the *in vivo* experiments. We would also like to thank Philipp Kainz (KML Vision GmbH) for technical input when compiling the manuscript. Figure 1e was created with BioRender.com.

Conflicts of Interest: The authors declare no conflict of interest. The funders had no role in the design of the study; in the collection, analyses, or interpretation of data; in the writing of the manuscript, or in the decision to publish the results.

References

[1] C. H. Foster, M. Karsy, M. R. Jensen, J. Guan, I. Eli, and M. A. Mahan, "Trends and Cost-Analysis of Lower Extremity Nerve Injury Using the National Inpatient Sample," *Neurosurgery*, vol. 85, no. 2, pp. 250–256, Aug. 2019, doi: 10.1093/neuros/nyy265.

[2] M. Karsy, R. Watkins, M. R. Jensen, J. Guan, A. A. Brock, and M. A. Mahan, "Trends and Cost Analysis of Upper Extremity Nerve Injury Using the National (Nationwide) Inpatient Sample," *World Neurosurg.*, vol. 123, pp. e488–e500, Mar. 2019, doi: 10.1016/j.wneu.2018.11.192.

[3] R. López-Cebral, J. Silva-Correia, R. L. Reis, T. H. Silva, and J. M. Oliveira, "Peripheral Nerve Injury: Current Challenges, Conventional Treatment Approaches, and New Trends in Biomaterials-Based Regenerative Strategies," *ACS Biomater. Sci. Eng.*, vol. 3, no. 12, pp. 3098–3122, Dec. 2017, doi: 10.1021/acsbiomaterials.7b00655.

[4] D. Grinsell and C. P. Keating, "Peripheral Nerve Reconstruction after Injury: A Review of Clinical and Experimental Therapies," *BioMed Research International*, vol. 2014. 2014. doi: 10.1155/2014/698256.

[5] J. C. Heinzel *et al.*, "Beyond the Knife—Reviewing the Interplay of Psychosocial Factors and Peripheral Nerve Lesions," *J. Pers. Med.*, vol. 11, no. 11, p. 1200, Nov. 2021, doi: 10.3390/jpm11111200.

[6] K. D. Bergmeister *et al.*, "Acute and long-term costs of 268 peripheral nerve injuries in the upper extremity," *PLOS ONE*, vol. 15, no. 4, p. e0229530, Apr. 2020, doi: 10.1371/journal.pone.0229530.

[7] O. van Hecke, S. K. Austin, R. A. Khan, B. H. Smith, and N. Torrance, "Neuropathic pain in the general population: A systematic review of epidemiological studies," *Pain*, vol. 155, no. 4, pp. 654–662, Apr. 2014, doi: 10.1016/j.pain.2013.11.013.

[8] D. Bouhassira, "Neuropathic pain: Definition, assessment and epidemiology," *Rev. Neurol. (Paris)*, vol. 175, no. 1–2, pp. 16–25, Jan. 2019, doi: 10.1016/j.neurol.2018.09.016.

[9] N. Torrance, B. H. Smith, M. I. Bennett, and A. J. Lee, "The Epidemiology of Chronic Pain of Predominantly Neuropathic Origin. Results From a General Population Survey," *J. Pain*, vol. 7, no. 4, pp. 281–289, Apr. 2006, doi: 10.1016/j.jpain.2005.11.008.

[10] K. R. Jessen, R. Mirsky, and A. C. Lloyd, "Schwann Cells: Development and Role in Nerve Repair," *Cold Spring Harb. Perspect. Biol.*, vol. 7, no. 7, p. a020487, Jul. 2015, doi: 10.1101/cshperspect.a020487.

[11] W. Daly, L. Yao, D. Zeugolis, A. Windebank, and A. Pandit, "A biomaterials approach to peripheral nerve regeneration: bridging the peripheral nerve gap and enhancing functional recovery," *J. R. Soc. Interface*, vol. 9, no. 67, pp. 202–221, 2012, doi: 10.1098/rsif.2011.0438.

[12] C. M. Nichols *et al.*, "Effects of motor versus sensory nerve grafts on peripheral nerve regeneration," *Exp. Neurol.*, vol. 190, no. 2, pp. 347–355, 2004, doi: 10.1016/j.expneurol.2004.08.003.

[13] M. Siemionow and G. Brzezicki, "Chapter 8 Current Techniques and Concepts in Peripheral Nerve Repair," in *International Review of Neurobiology*, vol. 87, Elsevier, 2009, pp. 141–172. doi: 10.1016/S0074-7742(09)87008-6.

[14] L. H. Poppler *et al.*, "Axonal Growth Arrests After an Increased Accumulation of Schwann Cells Expressing Senescence Markers and Stromal Cells in Acellular Nerve Allografts," *Tissue Eng. Part A*, vol. 22, no. 13–14, pp. 949–961, Jul. 2016, doi: 10.1089/ten.tea.2016.0003.

[15] M. Saheb-Al-Zamani *et al.*, "Limited regeneration in long acellular nerve allografts is associated with increased Schwann cell senescence," *Exp. Neurol.*, vol. 247, pp. 165–177, Sep. 2013, doi: 10.1016/j.expneurol.2013.04.011.

[16] L. G. Lanigan *et al.*, "Comparative Pathology of the Peripheral Nervous System," *Vet. Pathol.*, vol. 58, no. 1, pp. 10–33, Jan. 2021, doi: 10.1177/0300985820959231.

[17] J. Lang, "[On connective tissue and blood vessels of the nerves]," *Z. Anat. Entwicklungsgesch.*, vol. 123, pp. 61–79, 1962.

[18] H. Millesi, T. Hausner, R. Schmidhammer, S. Trattnig, and M. Tschabitscher, "Anatomical structures to provide passive motility of peripheral nerve trunks and fascicles," *Acta Neurochir. Suppl.*, vol. 100, pp. 133–135, 2007, doi: 10.1007/978-3-211-72958-8_28.

[19] P. Muangsanit, R. J. Shipley, and J. B. Phillips, "Vascularization Strategies for Peripheral Nerve Tissue Engineering: VASCULARIZATION STRATEGIES FOR NERVE TISSUE ENGINEERING," *Anat. Rec.*, vol. 301, no. 10, pp. 1657–1667, Oct. 2018, doi: 10.1002/ar.23919.

[20] M. I. Hobson, R. Brown, C. J. Green, and G. Terenghi, "Inter-relationships between angiogenesis and nerve regeneration: a histochemical study," *Br. J. Plast. Surg.*, vol. 50, no. 2, pp. 125–131, Feb. 1997, doi: 10.1016/S0007-1226(97)91325-4.

[21] A.-L. Cattin *et al.*, "Macrophage-Induced Blood Vessels Guide Schwann Cell-Mediated Regeneration of Peripheral Nerves," *Cell*, vol. 162, no. 5, pp. 1127–1139, Aug. 2015, doi: 10.1016/j.cell.2015.07.021.

[22] M. Caillaud, L. Richard, J.-M. Vallat, A. Desmoulière, and F. Billet, "Peripheral nerve regeneration and intraneural revascularization," *Neural Regen. Res.*, vol. 14, no. 1, p. 24, 2019, doi: 10.4103/1673-5374.243699.

[23] C. Prahm, J. Heinzel, and J. Kolbenschlag, "Blood Supply and Microcirculation of the Peripheral Nerve," in *Peripheral Nerve Tissue Engineering and Regeneration*, J. Phillips, D. Hercher, and T. Hausner, Eds. Cham: Springer International Publishing, 2020, pp. 1–46. doi: 10.1007/978-3-030-06217-0_21-1.

[24] F. Meng, X. Jing, G. Song, L. Jie, and F. Shen, "Prox1 induces new lymphatic vessel formation and promotes nerve reconstruction in a mouse model of sciatic nerve crush injury," *J. Anat.*, vol. 237, no. 5, pp. 933–940, Nov. 2020, doi: 10.1111/joa.13247.

[25] S. Sunderland, "THE CONNECTIVE TISSUES OF PERIPHERAL NERVES," *Brain*, vol. 88, no. 4, pp. 841–854, 1965, doi: 10.1093/brain/88.4.841.

[26] N. Volpi *et al.*, "Lymphatic vessels in human sural nerve: immunohistochemical detection by D2-40," *Lymphology*, vol. 39, no. 4, pp. 171–173, Dec. 2006.

[27] F. S. Frueh *et al.*, "A potential role of lymphangiogenesis for peripheral nerve injury and regeneration," *Med. Hypotheses*, vol. 135, p. 109470, Feb. 2020, doi: 10.1016/j.mehy.2019.109470.

[28] I. Zucal, D. Mihic-Probst, A.-L. Pignet, M. Calcagni, P. Giovanoli, and F. S. Frueh, "Intraneural fibrosis and loss of microvascular architecture — Key findings investigating failed human nerve allografts," *Ann. Anat. - Anat. Anz.*, vol. 239, p. 151810, Jan. 2022, doi: 10.1016/j.aanat.2021.151810.

[29] J. C. Heinzel *et al.*, "Evaluation of Functional Recovery in Rats After Median Nerve Resection and Autograft Repair Using Computerized Gait Analysis," *Front. Neurosci.*, vol. 14, p. 593545, Jan. 2021, doi: 10.3389/fnins.2020.593545.

[30] R. Kaewkhaw, A. M. Scutt, and J. W. Haycock, "Integrated culture and purification of rat Schwann cells from freshly isolated adult tissue," *Nat. Protoc.*, vol. 7, no. 11, pp. 1996–2004, Nov. 2012, doi: 10.1038/nprot.2012.118.

[31] T. Weiss, S. Taschner-Mandl, P. F. Ambros, and I. M. Ambros, "Detailed Protocols for the Isolation, Culture, Enrichment and Immunostaining of Primary Human Schwann Cells," in *Schwann Cells*, vol. 1739, P. V. Monje and H. A. Kim, Eds. New York, NY: Springer New York, 2018, pp. 67–86. doi: 10.1007/978-1-4939-7649-2_5.

[32] K. Schimek *et al.*, "Integrating biological vasculature into a multi-organ-chip microsystem," *Lab. Chip*, vol. 13, no. 18, p. 3588, 2013, doi: 10.1039/c3lc50217a.

[33] L. Knezevic *et al.*, "Engineering Blood and Lymphatic Microvascular Networks in Fibrin Matrices," *Front. Bioeng. Biotechnol.*, vol. 5, p. 25, 2017, doi: 10.3389/fbioe.2017.00025.

[34] E. Priglinger *et al.*, "Improvement of adipose tissue–derived cells by low-energy extracorporeal shock wave therapy," *Cytotherapy*, vol. 19, no. 9, pp. 1079–1095, Sep. 2017, doi: 10.1016/j.jcyt.2017.05.010.

[35] A. Suarez-Arnedo, F. T. Figueroa, C. Clavijo, P. Arbeláez, J. C. Cruz, and C. Muñoz-Camargo, "An image J plugin for the high throughput image analysis of in vitro scratch wound healing assays," *PLOS ONE*, vol. 15, no. 7, p. e0232565, Jul. 2020, doi: 10.1371/journal.pone.0232565.

[36] E. Zudaire, L. Gambardella, C. Kurcz, and S. Vermeren, "A computational tool for quantitative analysis of vascular networks," *PloS One*, vol. 6, no. 11, p. e27385, 2011, doi: 10.1371/journal.pone.0027385.

[37] S. M. Meadows *et al.*, "Integration of Repulsive Guidance Cues Generates Avascular Zones That Shape Mammalian Blood Vessels," *Circ. Res.*, vol. 110, no. 1, pp. 34–46, Jan. 2012, doi: 10.1161/CIRCRESAHA.111.249847.

[38] A. M. Ochsenbein, S. Karaman, G. Jurisic, and M. Detmar, "The Role of Neuropilin-1/Semaphorin 3A Signaling in Lymphatic Vessel Development and Maturation," in *Developmental Aspects of the Lymphatic Vascular System*, vol. 214, F. Kiefer and S. Schulte-Merker, Eds. Vienna: Springer Vienna, 2014, pp. 143–152. doi: 10.1007/978-3-7091-1646-3_11.

[39] K. Takeda, Y. Sowa, K. Nishino, K. Itoh, and S. Fushiki, "Adipose-Derived Stem Cells Promote Proliferation, Migration, and Tube Formation of Lymphatic Endothelial Cells In Vitro by Secreting Lymphangiogenic Factors," *Ann. Plast. Surg.*, vol. 74, no. 6, pp. 728–736, Jun. 2015, doi: 10.1097/SAP.0000000000000084.

[40] S. Landau *et al.*, "Investigating lymphangiogenesis in vitro and in vivo using engineered human lymphatic vessel networks," *Proc. Natl. Acad. Sci. U. S. A.*, vol. 118, no. 31, p. e2101931118, Aug. 2021, doi: 10.1073/pnas.2101931118.

[41] D. Huang *et al.*, "Schwann Cell-conditioned Medium Inhibits Angiogenesis1," *Cancer Res.*, vol. 60, no. 21, pp. 5966–5971, Nov. 2000.

[42] D. Huang *et al.*, "Schwann cell-conditioned medium inhibits angiogenesis in vitro and in vivo," *Med. Pediatr. Oncol.*, vol. 35, no. 6, pp. 590–592, Dec. 2000, doi: 10.1002/1096-911X(20001201)35:6<590::AID-MPO21>3.0.CO;2-O.

[43] A. Chlenski *et al.*, "SPARC Is a Key Schwannian-derived Inhibitor Controlling Neuroblastoma Tumor Angiogenesis1," *Cancer Res.*, vol. 62, no. 24, pp. 7357–7363, Dec. 2002.

[44] F. Peng *et al.*, "SPARC suppresses lymph node metastasis by regulating the expression of VEGFs in ovarian carcinoma," *Int. J. Oncol.*, vol. 51, no. 6, pp. 1920–1928, Dec. 2017, doi: 10.3892/ijo.2017.4168.